Journal Article

Octenyl-succinylated inulins for the delivery of hydrophobic drug

Han, L., Sun, J., Williams, P.A., Yang, J., Zhang, S.

Journal Pre-proof

Octenyl-succinylated inulins for the delivery of hydrophobic drug

Lingyu Han, Jiao Sun, Peter A. Williams, Jixin Yang, Shubiao Zhang

PII: S0141-8130(22)02000-1

DOI: https://doi.org/10.1016/j.ijbiomac.2022.09.068

Reference: BIOMAC 21943

To appear in: *International Journal of Biological Macromolecules*

Received date: 29 June 2022

Revised date: 12 August 2022

Accepted date: 7 September 2022

Please cite this article as: L. Han, J. Sun, P.A. Williams, et al., Octenyl-succinylated inulins for the delivery of hydrophobic drug, *International Journal of Biological Macromolecules* (2022), https://doi.org/10.1016/j.ijbiomac.2022.09.068

Octenyl-succinylated inulins for the delivery of hydrophobic drug

Lingyu Han[a, †], Jiao Sun[a, †], Peter A. Williams[b], Jixin Yang[b] and Shubiao Zhang[a,*]

[a] *Key Lab of Biotechnology and Bioresources Utilization of Ministry of Education, College of Life Science, Dalian Minzu University, Dalian, Liaoning, 116600, China;*

[b] *Faculty of Arts, Science and Technology, Wrexham Glyndwr University, Plas Coch, Mold Road, Wrexham, LL11 2AW United Kingdom.*

*Corresponding author: Professor Sunbiao Zhang, Key Lab of Biotechnology and Bioresources Utilization of Ministry of Education, College of Life Science, Dalian Minzu University, Dalian, Liaoning, 116600, China.

Tel: +86-0411-87656141

Email: zsb@dlnu.edu.cn

† These authors contributed equally to this work.

Abstract

The efficacy of hydrophobic anticancer drugs is limited by their poor solubility in water, inefficient target delivery, and toxic side effects. In this work, doxorubicin (DOX) was solubilized using OSA-inulins which created micellar aggregates in aqueous solution above a critical concentration. *In vitro* delivery of OSA-inulin-DOX micelles resulted in strong inhibition of the growth of MCF-7 breast cancer cells as compared to free DOX. They also displayed a faster cellular uptake rate, indicating that the micelles were promptly internalized into the cells through CD44 receptor-mediated endocytosis. During *in vivo* tumor suppression experiments in tumor-bearing mice, the OSA-inulin-DOX micelles strongly hindered tumor growth

and showed substantially lower systemic toxicity compared with free DOX. Our achievements demonstrate that OSA-inulin has great potential for the encapsulating, dissolving, and targeted delivery of hydrophobic drugs, especially antitumor drugs, for nutraceutical, medical, and pharmaceutical applications.

Keywords: Octenyl-succinylated inulin, encapsulation, release

1. Introduction

Chemotherapy is well-established as one of the most fundamental therapeutic mechanisms to inhibit tumor growth. Many antitumor drugs are hampered by poor water solubility, severe side effects, and/or non-selectivity [1]. There are plenty of strategies to overcome these problems of hydrophobic anticancer drugs, such as nanocarriers [2-4], self-amplifying nanodrugs [5], and self-sufficient bi-prodrug nanomedicine strategies [6], have been broadly explored as drug delivery tools. Biopolymer micelles are capable of improving the effectiveness of antitumor medications through enhancing their solubility and prolonging the circulation period in the bloodstream [7]. Furthermore, the accumulation of medications in tissues of the tumor has been ameliorated through enhanced permeability and retention (EPR) impact [8, 9] or by the use of antibodies, folic acid peptides, and many other functional molecules [10-13].

Inulin is a fructan-type polysaccharide, that is composed of (2→1) linked β-D-fructosyl-fructosyl residues with degrees of polymerization (DP) between 2-60, usually ending with an α-D-glucopyranosyl bond [14]. It is commonly used in food processing and is classified as a sort of dietary fiber since it is not absorbed in the

small intestine or stomach although passes through to the colon where is it degraded by bacterial enzymes to create short-chain fatty acids. Hydrophobic inulin derivatives, capable of forming micellar aggregates, have been synthesized in organic solvents by a number of researchers reacting inulin with methyl esters, fatty acid chlorides, alkyl isocyanates, and alkyl epoxides [15, 16]. We have previously reported studies on the synthesis of alkenyl succinylated inulin derivatives with a range of degrees of substitution (DS) and alkenyl chain lengths (C8-C18) prepared in aqueous solution under mild alkaline conditions, which have been shown to form micelle-like aggregates in solution [17-19]. We have also reported on the ability of alkenyl succinylated inulin derivatives to encapsulate beta-carotene and to evaluate its release under various solvent conditions [20, 21]. Maley et al. (2016) evaluated the ability of a commercially available hydrophobically-modified inulin derivative, i.e. Inutec SP1® to encapsulate and deliver the anticancer drug paclitaxel (PTX) *in-vivo*. The aim of the current study was to synthesise and characterize a number of octenyl succinylated inulin derivatives (OSA-inulin) using inulin samples of varying molar mass and to confirm their ability to encapsulate the anticancer drug doxorubicin, DOX. In addition the study includes an investigation of the kinetics of the release process, the ability to lower toxic side effects on MCF-7 cells and the effect on tumor growth *in vivo* through the delivery of DOX to tumor-bearing mice.

2. Materials and Methods

2.1. Materials

Inulin INUTEC® H25P was acquired from Beneo Biobased Chemicals. It was already identified employing Matrix-Assisted Laser Desorption Ionisation Time of Flight (MALDI-TOF) mass spectrometry and its DP was detected to lie between 2 and 8, in accordance with the information provided from the producers [22]. Fibruline (XL) and Fibruline® (DS2) were procured from Cosucra Chemicals. The DP of DS2 was determined to be 2-18 (Han, Ratcliffe & Williams, 2017) whilst the correspondent XL DP was 20-23 [23]. Prior to utilization, the inulin was dehydrated for 24 hours at 70 °C. Octenyl succinic anhydride (OSA) was acquired from Tokyo Chemical Industry UK Ltd, Oxford, and utilized as soon as it was received. Sudan IV and doxorubicin (DOX) were obtained from Shanghai Macklin Biochemical Co., Ltd. Cell Counting Kit-8 (CCK-8) and DAPI were procured from Shanghai Beyotime Biotechnology Co. Ltd. Fetal bovine serum (FBS) and Dulbecco's modified Eagle medium (DMEM) were acquired from Gibco BRL (Bethesda, MD, USA). The cells of human breast cancer (MCF-7) were procured from the Institute of Biochemistry and Cell Biology (China). 4-6 weeks old female BALB/c nude mice were procured from the Beijing Vital River Laboratory Animal Technology Co., Ltd. (Beijing, China). Analytical grade was employed for all other chemicals.

2.2. Methods

2.2.1. Synthesis

Octenyl succinylated deriviatives of DS2, H25P and XL inulins were prepared in aqueous solution under alkaline circumstances as already described [19].

2.2.2. NMR spectroscopy

The spectra of ^{1}H-NMR for the OSA-inulins were procured according to the previous report [19] employing a 500 MHz NMR spectrometer (SANTAK Mercury plus 400) at 25 °C. Briefly, 5 mg of specimen in 0.7 g of D_2O at 40 °C was dissolved and then transferred to a 5 mm thin wall tube of NMR for the measurement. The spectra of ^{1}H-NMR were evaluated at 25 °C employing a 500 MHz magnet. For all samples, sixteen scans were conducted. The Pulse Program ZG30 with a 30-degree pulse and a delay of 1 s was implemented simultaneously with Mnova 7.0 computer program.

2.2.3. Fourier-transform infrared spectroscopy (FTIR)

The spectra of FTIR for OSA-inulin samples were obtained as already reported [19]. The samples of OSA-inulin were dehydrated at 70 °C in an oven overnight. Next, 1 mg of specimen was milled with 100 mg of dehydrated KBr employing a pestle and agate mortar for a couple of minutes in order to obtain a desirable powder. By implementing a 15-ton manual press and a P/N 03000 13 mm pellet die (maximum load 10.0 tons) from Specac Limited, a thin pellet was created. The spectra of FTIR were obtained in the range 4000-400 cm^{-1} employing a Shimadzu AIM-8800 FTIR spectrometer running 16 scans at a resolution of 4 cm^{-1}. Spectral assessment and presentation were executed by implementing the interactive Perkin-Elmer Read-IR3 version 3.0 computer program.

2.2.4. Dye solubilization

The critical aggregation concentration (CAC) was determined employing a previously described dye solubilization technique [19] using Sudan IV. The preparation of a 1%

OSA-inulin stock solution was fulfilled and then diluted to create a range of concentrations. Sudan IV (5 mg) was then added to 5 mL of OSA-inulin solution at different concentrations and agitated at 40 °C overnight. Subsequently, the solutions were filtered to eliminate insoluble particles of Sudan IV by employing a Millex-GP 0.22 μm filter (Millipore Ireland, Ltd), into disposable UV grade 10 mm pathlength cuvettes (CXA-110-0053 from Fisher Scientific Ltd). For each solution, the absorbance was obtained at a wavelength of 510 nm with the aid of a UV/Vis Spectrometer (Shimadzu UV-2700). From the point at which the absorbance was first enhanced, the CAC was assessed.

2.2.5. Transmission Electron Microscopy (TEM)

Transmission electron microscopy (TEM) was executed by dropping 10 μL of liquid sample (OSA-inulin micelles or OSA-inulin-DOX drug-loaded micelles) on a carbon-coated copper grid, allowing 20-30 minutes to fully deposit the micelles on the carbon film of the copper mesh. By using a filter paper, the excess sample was removed. The copper grids were gradually dehydrated at 25 ± 1 °C for 2 h in a desiccator and then negatively stained with the help of phosphotungstic acid (10 mg/mL) for 60 s. The findings of the morphology of the micelles were obtained using a JOEL JEM-2100 transmission electron microscope.

2.2.6. Zeta potential

The zeta potential of the OSA-inulin samples was assessed by employing a nanoparticle size analyzer (HORIBA SZ-100). An aqueous sample solution at a concentration of 1% was prepared after stirring in a 40 °C water bath. A 0.22 μm

water-based membrane was used to evenly disperse the solution. The micelles were sealed and held at 4 °C for later utilization. An aliquot (2 mL) of the micelle solution was inserted into a four-way cuvette to measure the zeta potentials of H25P, DS2, and XL control micelles and H25P-DOX, DS2-DOX, and XL-DOX drug-loaded micelles with a nanolaser particle size analyzer. Each sample was measured in triplicate.

2.2.7. Encapsulation Efficiency and Drug Loading

For the appraisal of the drug loading (DL) and encapsulation efficiency (EE), 1 mL of DOX-containing sample solution (1.0 mg/mL) and 9 mL of chromatographic methanol were blended evenly and ultrasonically treated in a water bath for 15 minutes to destroy their structure. A UV/vis spectrophotometer was utilized to appraise the absorbance value of the sample at 495 nm, and a calibration curve of DOX was generated to calculate the DOX content in the micelles. Equations (1) and (2) were used to obtain the EE and DL of DOX-loaded OSA-inulin micelles.

$$\text{EE}\ (\%) = \frac{\text{weight of DOX in micelles}}{\text{weight of DOX fed initially}} \times 100 \quad (1)$$

$$\text{DL}\ (\%) = \frac{\text{weight of DOX in micelles}}{\text{weight of polymeric micelles containing DOX}} \times 100 \quad (2)$$

2.2.8. Hemolysis test

Murine red blood cells (RBC) were used to study the hemolysis activity of OSA-inulin blank micelles. First, fresh murine plasma was defibrated and then 8 mL of phosphate-buffered saline (PBS) (pH 7.4) was increased succeeded by centrifugation for 10 min at 1800 r/min. The plasma was removed and this procedure was repeated three times until the supernatant became colorless. The suspension of RBC was diluted with PBS to about 2% (v/v) and mixed by vortexing for 5 min. Next,

the diluted RBC suspension (1 mL) was mixed with OSA-inulin micelles (final concentrations 0.1 to 2.0 mg/mL) or with Tween 80 as a control. Following incubation in a constant temperature shaker at 37 °C for 3 h, the intact RBCs were eliminated through centrifugation for 10 min at 5000 r/min. A UV/vis spectrophotometer was used to detect the absorbance of the supernatant at 541 nm. Meanwhile, as the positive and negative controls in this experiment, 1 mL of RBC suspension was mixed with ultrapure water or PBS, respectively, and processed as described above. The assessments were executed three times in parallel, and the degree of hemolysis was evaluated employing Eq. (3).

$$Hemolysis\ rate\ (\%) = \frac{A_{test} - A_{neg}}{A_{POS} - A_{neg}} \times 100 \quad (3)$$

where A_{test} represents the absorbance value of the specimen; A_{neg} implies the absorbance value of the negative control (PBS) and A_{pos} implies the absorbance value of the positive control (water).

2.2.9. In vitro cytotoxicity of the micelles

The cytotoxicity of micelles towards MCF-7 cells was ascertained by the CCK-8 approach. Cells were added to a plate containing 96 wells at a density of 5×10^3 cells per well and transferred to a cell incubator for 24 h. A 1% sample solution was diluted with DMEM medium to prepare solutions of different concentrations. The cell medium was replaced with a complex solution of different concentrations and placed in an incubator for 72 h. Afterwards, to each well 10 μL of the solution of CCK-8 were added, mixed well, and transferred to the incubator for an additional 2 h. A UV/vis spectrophotometer (Shimadzu UV-2700) was implemented for detecting the

absorbance value of each well at the wavelength of 450 nm. The data were employed to assess the survival rate of the cell (the absorbance value of the experimental group accounts for a percentage of the absorbance value of the control group).

2.2.10. In vitro Cellular Uptake

The cells of MCF-7 were seeded on a glass-bottomed confocal dish and incubation was conducted for 24 h under 5% CO_2 at 37 °C. The free DOX or OSA-inulin-DOX solutions were mixed with DMEM medium to obtain a composite solution with an ultimate DOX concentration of 2.5 μg/mL. The cell suspensions (2 mL) were added to a confocal dish, transferred to an incubator, and incubated for 0.5 h, 2 h, or 4 h. Next, the milieu was eliminated, and the cells were rinsed three times by utilizing PBS (pH 7.4) to fully eliminate the DOX or drug-loaded micelles that had not entered the cells. Then, 500 μL 4% paraformaldehyde was added to each confocal dish at ambient temperature and incubated for 20 min to fix the cells, followed by three washes with PBS. Finally, the nuclei were stained by employing 200 μL DAPI for 10 min in the dark and subsequently rinsed three times with PBS. Fluorescent images were achieved employing an OLYMPUS FV10-ASW laser confocal microscope.

Subsequently, the cells of MCF-7 were seeded on a plate containing 12 well at a cell density of 2×10^4 per well for quantitative evaluation of the cellular uptake of micelles. After 24 hours of incubation, the cells reached about 80% confluence. Following incubation for 0.5 h, 2 h, or 4 h with free DOX or drug-loaded micelles with an ultimate concentration of DOX of about 2.5 μg/mL, the cells were rinsed three times by implementing PBS, digested with trypsin, pipetted, collected, and

filtered. The PE channel of the flow cytometer (FCM) was selected for detection and employed to quantitatively assess the fluorescence intensity of DOX in the cells.

2.2.11. *In vivo* antitumor study

BALB/c nude mice（110011211103064927）were employed as an animal model to study the *in vivo* antitumor effect of DOX-containing inulin micelles. The animal assessments and surgeries were exerted in compliance with the benchmarks of the Ethics Committee Approved Protocol (ID AEE20040) of Dalian Medical University, China. In this approach, five experimental groups were set up: normal saline, free DOX, H25P-DOX, DS2-DOX, and XL-DOX. The number of mice in each group was five, and the mice were injected with drugs within the tail vein every two days. The DOX equivalent concentration injected was 3.0 mg/kg and the mice injected with physiological saline were set as the blank control group. The weight of each mouse was determined every two days and a vernier caliper was applied to evaluate the long (L) and short (W) diameters of the tumor, and its volume was assessed as Tumor volume = $(W)^2 \times L/2$, to evaluate the tumor suppression efficiency *in vivo*.

2.2.12. *In vivo* safety study

Following administration, blood was withdrawn after anesthesia, and routine blood tests were performed comprising red blood cells (RBC), hemoglobin (HGB), white blood cells (WBC), and platelets (PLT). Furthermore, serum was obtained by centrifugation and tested for indicators comprising aspartate aminotransferase (AST), creatinine (CRE), alanine aminotransferase (ALT), and urea nitrogen (BUN). At the final stage of the assessment, the mice were killed, and the spleen, liver, heart, kidney,

lung, and tumor tissues were removed, rinsed with PBS, and fixed in the solution of 4% paraformaldehyde. The fixed tumors and organs were placed in paraffin and sliced into blank sections. Then the sections were stained by the solution of hematoxylin-eosin (H&E), observed, and photographed with an inverted fluorescence microscope.

2.2.13. *In vivo* imaging

Animal imaging assessments were exerted on 6-8-week-old BALB/c nude mice. Subcutaneous injection of about 1×10^6 MCF-7 cells was executed into the armpit of BALB/c nude mice. The mice were haphazardly categorized into five groups when the tumor volume became 80-100 mm^3. Each group was injected with normal saline, free DOX, H25P-DOX, DS2-DOX, or XL-DOX through the tail vein. The equivalent dose of DOX was 3.0 mg/kg. Pictures were taken with a bioluminescence IVIS imaging system (Xenogen, USA) 4 h and 24 h following injection, at 475 nm to assess the fluorescence distribution.

2.2.14. Statistical assessment

The outcomes were given as mean values ± SD. By employing two-way assessment of variance, the statistical significance was ascertained. P values < 0.05 were regarded statistically meaningful.

3. Results and discussion

3.1. Characterization of OSA-inulins

The DS values (expressed as moles of OSA per mole of fructose) of the altered

OSA-inulins (H25P, DS2, and XL) are exhibited in the Supplementary data Figure S1. The number of alkyl chains incorporated into the specimens was evaluated from the ratio of the peak area at 0.8 ppm to the area between 3.20-4.25 ppm (Table 1) as already explained [23]. The DS, expressed as moles of OSA per mole of fructose, were very similar for all the three OSA-inulins (DS2, H25P, and XL) with various DPs. The DS value of the OSA-inulins was around 33% which was higher than that in our previous study [20]. The spectra of FTIR for the OSA-inulin and unmodified inulin specimens are exhibited in Supplementary Data Figure S2 and were similar to our previously published work [17, 19].

The values of UV/vis absorbance achieved for the OSA-inulins in the presence of Sudan IV are provided in Supplementary data Figure S3. Echoing our previous research, the absorbance values first increased substantially above the critical concentration which is ascribed to the creation of micellar–like aggregates and the dissolution of the dye in the hydrophobic core [19]. The values of CAC for all the OSA-inulins in this work are shown in Table 1. Generally, the CAC decreased as the DP increased. The inulin sample with the greatest molar mass (inulin-XL) created micellar aggregations at a lowest concentration (0.02%) compared to the other inulins (0.06% for H25P and 0.04% for DS2). This may be due to the higher number of alkenyl chains per molecule for XL inulin with the distribution of the groups of octenyl along the chains of inulin could be a criterion as well. The values are generally comparable to those previously reported namely, 0.06% for OSA-modified inulin with a DS of ~29% [19] and an order of magnitude lesser than the values of

0.7-0.9% reported for OSA-modified inulin with DS 4-7% [17].

3.2. Characterization of OSA-inulin and OSA-inulin -DOX micelles.

The morphological structures of the micelles were scrutinized through TEM. As shown in Fig. 1A, the three polymers and their corresponding drug-loaded micelles were all globular in shape in agreement with previous results [21], and the particle size of the micelles did not exceed 100 nm. The micelles were much smaller than Inutec SP1® micelles (302.86 ±10.9 nm) and the paclitaxel-loaded Inutec SP1® micelles (256.37±10.9 nm) determined by TEM [25]. Interestingly, it has been reported that octenyl succinic anhydride-modified short glucan chains (OSA-SGC) mainly formed micelles or ultrasmall micelles around 30-40 nm in size by TEM [26]. The scale of the drug-loaded micelles was a little larger compared with the scale of the polymer micelles in the absence of DOX. This may be due to the fact that DOX has entered the inner core of the micelle, making the hydrophobic area larger and leading to an enhancement in the particle size of the micelle.

The zeta potentials of the OSA-inulin micelles with and without DOX encapsulated are presented in Fig. 1B and Table 1. The zeta potentials of the OSA-inulin micelles were negative, and the charge became less negative following the DOX loading. The negative charge of OSA-inulins is due to the presence of free carboxyl group. The CAC decreases as the DP increases from Supplementary data Figure S3 and Table 1, that is to say the number of aggregates decreases. Hence the number of carboxylate groups of aggregates reduces leading to the zeta potential decrease. DOX contains amino groups in its structure and is positively charged under

physiological conditions, therefore, the OSA-inulin micelles with DOX encapsulated show a lower negative charge compared to the OSA-inulin micelles. The larger XL inulin chains contain a greater number of alkenyl groups per chain which may facilitate enhanced intermolecular hydrophobic association in solution.

The drug loading (DL) and encapsulation efficiency (EE) ability of the different OSA-inulin samples are reported in Fig. 1C and Table 1. It is evident that as the inulin chain length increased, both the DL and EE of the micelles increased, which shows the same trend as in our previous report [21]. The increase in DL and EE helps reduce drug loss, improve drug efficacy, and reduce the cost of preparing drug-loaded micelles.

3.3. Cytotoxicity of the OSA-inulin micelles and hemolysis test

Since the amphiphilic polymers might damage the cell membrane, a hemolysis assessment was performed for the evaluation of the compatibility of their blood. When the material is hemolytic, it is able to rupture the membrane of red blood cells and release intracellular hemoglobin. The rate of hemolysis was therefore evaluated through assessing the absorbance of hemoglobin. As tween 80 has a strong damaging effect on cell membranes, it is often used as a reference to evaluate the hemolytic properties of materials [27]. As shown in Figs 2A and 2B, when the concentration of Tween 80 was enhanced from 0.1 to 2.0 mg/mL, the hemolysis rate was close to 100%. However, at 2.0 mg/mL all polymers in this study showed a hemolysis rate of no more than 4.0%, indicating that the prepared materials were essentially non-hemolytic. Generally, when the hemolysis rate of a carrier material is less than

5%, it is suitable for applications in the biomedical field [28]. The results confirmed that the OSA-inulin polymers have good biocompatibility and cause little damage to the cell membrane.

According to Fig. 2C, the survival rate of MCF-7 cells upon 72 h incubation in the presence of OSA-inulin micelles at a concentration of 25 to 500 μg/mL was superior to 90%. This demonstrated that OSA-inulin micelles possessed little cytotoxicity towards MCF-7 cells and were suitable as delivery vehicles for anti-tumor medications. The inhibition of growth of MCF-7 cells by free DOX or drug-loaded polymers was characterized by their IC_{50}. As shown in Supplementary data Figure S4 and Fig. 2C, the IC_{50} values of free DOX, H25P-DX, DS2-DOX, and XL-DOX are 0.119, 0.109, 0.101, and 0.097 μg/mL, accordingly, demonstrating that the growth inhibitory effect of OSA-inulin-DOX micelles, which followed the order of H25P<DS2<XL, reflected their molar masses and was a bit superior to that of free DOX. Therefore, the drug loaded OSA-inulin micelles show an improved *in vitro* therapeutic effect compared with free DOX. This may be due to the fact that the size of the polymer conforms to the enhanced permeability and retention (EPR) impact [29], which enhances the uptake of drug-loaded micelles by the cells. In addition, based on our previous research, the OSA-inulin micelle is very sensitive to low pH values (Han *et al*., 2020), hence it can quickly release DOX from lysosomes, which can improve the cell growth inhibitory effect of the micelles.

3.4. In vitro cellular uptake

The absorption of free DOX and OSA-inulin-DOX micelles in MCF-7 cells was

scrutinized quantitatively employing flow cytometry (FCM) and confocal laser scanning fluorescence microscopy (CLSM). The incubation of MCF-7 cells was fulfilled with free DOX, H25P-DOX, DS2-DOX, and XL-DOX for 4 hours. As shown in Fig. 3A, after 0.5 hours incubation, the cellular uptake rates of H25P-DOX, DS2-DOX, and XL-DOX micelles into MCF-7 cells were 9.8%, 10.5%, and 11.7%, respectively, which reflected their molar masses for instance H25P<DS2<XL. All OSA-inulin-DOX micelles showed a higher DOX uptake rate compared with the cells incubated with free DOX (2.5%). Following 2 hours of incubation with XL-DOX micelles, the rate of uptake for DOX into MCF-7 cells reached 99.4%, which was 5.9% superior to that of free DOX. The cellular uptake rate of the micelles into MCF-7 was further enhanced after 4 hours of incubation, demonstrating that, in contrast to free DOX, the OSA-inulin-DOX micelles were continuously taken up via the MCF-7 cells, which meant that the cellular uptake enhanced in a time-dependent behavior.

Following incubation of MCF-7 cells with free DOX, H25P-DOX, DS2-DOX, or XL-DOX for 0.5 hours, 2 hours, and 4 hours, CLSM images were obtained as demonstrated in Fig. 3B. At 0.5 h, the red fluorescence of DOX was detected in various groups, exhibiting that all free DOX and OSA-inulin-DOX micelles were effectively taken up via the cells of MCF-7. However, cells incubated with OSA-inulin-DOX micelles demonstrated more potent DOX fluorescence in comparison to the cells incubated with free DOX in both nucleus and cytoplasm, illustrating that delivery of DOX to the cytoplasm by OSA-inulin micelles (*via* CD44 receptor-mediated endocytosis) was more efficient than the delivery of free DOX. We

also found that the intensity of intracellular fluorescence was considerably ameliorated following 2 hours and 4 hours of incubation, indicating that the OSA-inulin-DOX micelles can be constantly taken up into MCF-7 cells and the cellular adsorption enhanced in a time-dependent behavior. The observations of OSA-inulin-DOX micelles using CLSM are in good agreement with the cell uptake results according to FCM. Gao *et al*. [3] described how the pH-responsiveness of polymers resulted in a rapid release of DOX. Our previous results [21] indicated that OSA-inulins (H25P, DS2, and XL) are very sensitive to changes in the pH, which could be the main reason for the rapid release of DOX from OSA-inulin-DOX micelles in the acidic microenvironment of cancer cells.

3.5. In vivo antitumor effect

We next investigated the *in vivo* antitumor influence of the DOX-containing micelles. To this end, nude mice were injected with MCF-7 cells to form tumors. When the tumors were around 100 mm^3 in size, the mice were administered with DOX or various DOX-containing micelles, with saline as control group. Tumor volumes were measured every other day following the start of treatment. A tumor volume-time curve was drawn for additional illustration of the tumor-suppressive effect of micelles (Fig. 4A and 4B). The pictures of mice, tumors, and different organs at the end of the treatment are shown in Figure S5. After 30 days of drug administration, mice injected with drug-loaded micelles and free DOX achieved a tumor inhibition rate of about 80% or more compared with the saline group. The greatest anti-tumor effect was observed upon treatment of the mice with the XL-DOX micelles (Figs 4A and 4B). This

achievement is in agreement with the *in vitro* tumor suppressor evaluation in MCF-7 cells and may be due to XL-DOX having the longest chain length and a higher cellular uptake rate under the same concentration.

In addition, it was found that at the end of treating, the bodyweight of mice in the group of free DOX was lesser than that of the mice in the other groups (Fig. 4C), while there existed no substantial discrepancy between the DOX-micelle groups and the saline control group. Meanwhile, it was detected that the tumor weight of mice in the drug administration groups was less than that of the group of control, with the XL-DOX group being the lowest, suggesting that XL-DOX gave the best treatment effect (Fig. 4E). Moreover, the degree of tumor weight inhibition (TWI) was evaluated from tumor weights with the equation: $TWI(\%)= (W_A - W_B)/W_A \times 100$ [30], where W_A and W_B demonstrate the mean tumor weights of mice processed with saline in the control group and diverse formulations comprising DOX, accordingly. Consistent with the last achievements of tumor volume assessments, XL-DOX micelles obtained the greatest TWI (96.98%), succeeded by DS2-DOX (94.55%) and H25P-DOX (91.21%), while TWI of the free DOX group was 86.46%. Likewise, the weights of the liver and spleen of mice in the group of free DOX were lesser than those in the other groups, indicating that long-term injection of free DOX damaged these organs (Fig. 4F).

Furthermore, we performed *in vivo* imaging of tumors of mice treated with DOX-containing micelles 4 hours and 24 hours following tail vein injection. The results (Fig. 4D) showed that drug-loaded micelles displayed a greater accumulation

at the tumor site compared with free DOX. At 4h, both drug-loaded and free DOX micelles accumulated in the liver, while at 24h, DOX accumulation in the liver of mice from the free DOX group was more prominent. The decreased fluorescence intensity of drug-loaded micelles in the liver may be due to their well-hydration *in vivo*. It inhibited the recognition of macrophages in the reticuloendothelial system through the EPR effect, resulting in prolonged circulation in the blood and more accumulation in tumors. The fluorescence of XL-DOX at the tumor site was slightly more potent than that of other groups at 24 h, which is consistent with the results of tumor suppression rate *in vivo*. Therefore, the OSA-inulin micelles, having remarkably low toxicity and excellent release of DOX in tumors, illustrated excellent benefits over free DOX.

3.6. In vivo safety evaluation

We next carried out an *in vivo* safety evaluation of the OSA-inulin-DOX micelles. Biochemical blood tests determining liver and kidney function showed that, in comparison to the saline group, the aspartate aminotransferase (AST), creatinine (CRE), alanine aminotransferase (ALT), and urea (BUN) levels of the DOX groups fluctuated, with the largest increase in the free DOX group (Fig. 5A). Free serum DOX has a certain level of toxicity. Although the routine blood test results of the other groups were affected by the administration of DOX, the change in the reference interval at this dose was still safe (Fig. 5A). The results of routine blood tests showed that the red blood cells (RBC), platelets (PLT), white blood cells (WBC), and hemoglobin (HGB) of the OSA-inulin-DOX micelles changed in a certain range , but

for the free DOX group these indicator increased greatly (Fig. 5B).

Next, hematoxylin and eosin (H&E) slices were prepared from the tumor tissue and other organs and observed under an inverted fluorescence microscope. The tumor tissue slices in the saline group revealed many mitotic cells, while the cells from the treatment groups showed signs of separation from surrounding cells. This indicated that, while the tumors of the saline group were proliferating rapidly, the growth of tumors of the administration group was inhibited. In the tissue sections of the liver and spleen in the free DOX group, pathological damage was observed, including extensive vacuolar degeneration of hepatocytes (Fig. 5C). The slices of liver and spleen from mice of the H25P-DOX, DS2-DOX, and XL-DOX groups were similar in health to the saline control group, further confirming that DOX-loaded micelles lowered the damage of DOX to organs. Overall, the *in vivo* tumor suppression experiments illustrated that the DOX-loaded micelles represented better anti-tumor activity and lower toxic side effects than free DOX, indicating their great potential in anti-tumor drug delivery systems. We verified that the OSA-inulin micelles, especially XL-DOX, potently encapsulated and transported hydrophobic DOX to tumors, whilst inhibiting undesirable leakage of drug into the systemic circulation. When the micelles reached the tumor cells, the EPR effects enhanced the uptake of drug-loaded micelles by the cells. The resulting platform displayed significantly enhanced anticancer efficiency whilst maintaining insignificant side effects.

4. Conclusions

OSA-inulins, prepared using inulin of varying DP, formed micelles in solution above the critical concentration. And we demonstrated that DOX was capable of promptly being encapsulated in the hydrophobic cores of the micellar aggregations for ameliorated antitumor delivery. The EE and DL capability was greatest for XL modified inulin among OSA-inulins. *In vitro* investigations illustrated that the negatively charged OSA-inulin micelles represented tremendous stability and negligible cytotoxicity in serum. The OSA-inulin-DOX micelles exhibited enhanced cellular uptake and strong cell growth inhibition. The improved antitumor effect of OSA-inulin-DOX micelles compared with free DOX in both *in vivo* and *in vitro* investigations. Importantly, OSA-inulin-DOX micelles exhibited remarkably reduced toxic and side effects on organs compared with free DOX. Therefore, OSA-inulin has considerable capability for tumor specificity and fast delivery of homologous hydrophobic medications for improved anticancer efficacy. It has great potential for medical applications of targeted drug delivery.

Acknowledgments

This work was supported by the National Natural Science Foundation of China (No. 31701555), the National High-Tech Research and Development Program of China (863 Program, 2014AA020707), the National Natural Science Foundation of China (21503035, 21606041, and 21776044), the Fundamental Research Funds for the Central Universities, the Natural science foundation of Liaoning province (2021-MS-147), the Dalian high-level talent innovation, scientific and technological talent entrepreneurship and innovation team support projects in key fields

(2020RQ122).

References

1. J. Shi, P.W. Kantoff, R. Wooster, O.C. Farokhzad, Cancer nanomedicine: progress, challenges and opportunities. *Nat. Rev. Cancer 17*(2016)20.

2. F. Dosio, S. Arpicco, B. Stella, E. Fattal, Hyaluronic acid for anticancer drug and nucleic acid delivery. *Adv. Drug Del. Rev. 97*(2016)204-236.

3. Q.Q. Gao, C.M. Zhang, E.X. Zhang, H.Y. Chen, Y.H. Zhen, S.B. Zhang, S.F. Zhang, Zwitterionic pH-responsive hyaluronic acid polymer micelles for delivery of doxorubicin. *Coll. Surf B Biointerf. 178*(2019)412-420.

4. Z. Wang, G. Ma, J. Zhang, W. Lin, F. Ji, M.T. Bernards, S. Chen, Development of Zwitterionic Polymer-Based Doxorubicin Conjugates: Tuning the Surface Charge To Prolong the Circulation and Reduce Toxicity. *Langmuir. 30*(2014)3764-3774.

5. S. Zhou, Q. Shang, N. Wang, Q. Li, A. Song, Y. Luan, Rational design of a minimalist nanoplatform to maximize immunotherapeutic efficacy: Four birds with one stone. *Journal of controlled release. 328*(2020)617-630.

6. M. Zhang , X. Qin , Z. Zhao , Q. Du , Q. Li , Y. Jiang, Y. Luan, A self-amplifying nanodrug to manipulate the Janus-faced nature of ferroptosis for tumor therapy. *Nanoscale Horizons. 7*(2022)198-210.

7. K.F. Liu, Y.X. Liu, C.X. Li, L.Y. Wang, J. Liu, J.D. Lei, Self-Assembled pH and Redox Dual Responsive Carboxymethylcellulose-Based Polymeric Nanoparticles for Efficient Anticancer Drug Codelivery. *ACS Biomater. Sci. Eng. 4*(2018)4200-4207.

8. H. Maeda, H. Nakamura, J. Fang, The EPR effect for macromolecular drug delivery to solid tumors: Improvement of tumor uptake, lowering of systemic toxicity, and distinct tumor imaging in vivo. *Adv. Drug Del. Rev. 65*(2013)71-79.

9. H. Nakamura, F. Jun, H. Maeda, Development of next-generation macromolecular drugs based on the EPR effect: challenges and pitfalls. *Exp. Opin. Drug Del. 12*(2015)53-64.

10. A. Cimini, B. D'Angelo, S. Das, R. Gentile, E. Benedetti, V. Singh, S. Monaco, S. Santucci, S. Seal, Antibody-conjugated PEGylated cerium oxide nanoparticles for specific targeting of Aβ aggregates modulate neuronal survival pathways. *Acta Biomater. 8*(2012)2056-2067.

11. J. Gu, X. Chen, X. Ren, X. Zhang, X. Fang, X. Sha, CD44-Targeted Hyaluronic Acid-Coated Redox-Responsive Hyperbranched Poly(amido amine)/Plasmid DNA Ternary Nanoassemblies for Efficient Gene Delivery. *Bioconj. Chem. 27*(2016)1723-1736.

12. X. Li, X. Yang, Z. Lin, D. Wang, D. Mei, B. He, X. Wang, X. Wang, Q. Zhang, W. Gao, A folate modified pH sensitive targeted polymeric micelle alleviated systemic toxicity of doxorubicin (DOX) in multi-drug resistant tumor bearing mice. *Eur. J. Pharm. Sci. 76*(2015)95-101.

13. K.N. Sugahara, G.B. Braun, T.D. Mendoza, V.R. Kotamraju, R.P. French, A. Lowy, T. Teesalu, E. Ruoslahti, Tumor-Penetrating iRGD Peptide Inhibits Metastasis. *Molecular cancer therapeutics, 14*(2015)120-128.

14. A.D. French, Recent Advances in the Structural Chemistry of Inulin. *Studies in*

Plant Science, 3(1993)121-127.

15. C.V. Stevens, A. Meriggi, M. Peristeropoulou, P.P. Christov, K. Booten, B. Levecke, A. Vandamme, N. Pittevils, T.F. Tadros, Polymeric Surfactants Based on Inulin, a Polysaccharide Extracted from Chicory. 1. Synthesis and Interfacial Properties. *Biomacromolecules 2*(2001)1256.
16. D. Exerowa, G. Gotchev, T. Kolarov, K. Kristov, B. Levecke, T. Tadros, Comparison of oil-in-water emulsion films produced using ABA or AB n copolymers. *Colloids & Surfaces A Physicochemical & Engineering Aspects, 335*(2009)50-54.
17. S. Kokubun, I. Ratcliffe, P. Williams, Synthesis, characterization and self-assembly of biosurfactants based on hydrophobically modified inulins. *Biomacromolecules 14*(2013)2830-2836.
18. S. Kokubun, I. Ratcliffe, P. Williams, The emulsification properties of octenyl- and dodecenyl- succinylated inulins. *Food Hydrocolloids, 50*(2015)145-149.
19. L. Han, I. Ratcliffe, P.A. Williams, Self-assembly and emulsification properties of hydrophobically modified inulin. *J Agric Food Chem, 63*(2015)3709-3715.
20. S. Kokubun, I. Ratcliffe, P.A. Williams, The interfacial, emulsification and encapsulation properties of hydrophobically modified inulin. *Carbohydr Polym, 194*(2018)18-23.
21. L. Han, B. Hu, I. Ratcliffe, C. Senan, J. Yang, P. Williams, Octenyl-succinylated inulin for the encapsulation and release of hydrophobic compounds. *Carbohyd. Polymers 238*(2020)116199.

22. M. Evans, J.A. Gallagher, I. Ratcliffe, P.A. Williams, Functional properties of hydrophobically modified inulin in *Gums and Stabilisers for the Food Industry 17*, Proceedings of the Gums and Stabilisers for the Food Industry Conference, June 25−28, 2013, Glyndwr University, Wales, U.K. ; Williams, P.A., Philips, G.O., Eds., Royal Society of Chemistry Special Publication No. 346; CPI Group: Croydon, U.K., 2014; pp 73−78.

23. S.N. Ronkart, C. Deroanne, M. Paquot, C. Fougnies, J. Lambrechts, C. Blecker, Characterization of the Physical State of Spray-Dried Inulin. *Food Biophys. 2*(2007)83-92.

24. L. Han, I. Ratcliffe, P.A. Williams, Synthesis, characterisation and physicochemical properties of hydrophobically modified inulin using long-chain fatty acyl chlorides. *Carbohyd. Polymers 178*(2017)141-146.

25. P. Muley, S. Kumar, F. El Kourati, S.S. Kesharwani, H. Tummala, Hydrophobically modified inulin as an amphiphilic carbohydrate polymer for micellar delivery of paclitaxel for intravenous route. *International Journal of Pharmaceutics, 50*(2016)32-41.

26. R. Chang, J. Yang, S. Ge, M. Zhao, C. Liang, L. Xiong, Q. Sun, Synthesis and self-assembly of octenyl succinic anhydride modified short glucan chains based amphiphilic biopolymer: Micelles, ultrasmall micelles, vesicles, and lutein encapsulation/release. *Food Hydrocolloids, 67*(2017)14-26.

27. K. Seo, D. Kim, pH-dependent hemolysis of biocompatible imidazole-grafted polyaspartamide derivatives. *Acta Biomaterialia, 6*(2010)2157-2164.

28. S. Yadav, S. Majumdar, A. Ali, S. Krishnamurthy, P. Singh, R. Pyare, In-vitro analysis of bioactivity, hemolysis, and mechanical properties of zn substituted calcium zirconium silicate (baghdadite). *Ceramics International*, *47*(2021)16037-16053.

29. H. Maeda, The enhanced permeability and retention (EPR) effect in tumor vasculature: the key role of tumor-selective macromolecular drug targeting. *Adv Enzyme Regul*, *41*(2001)189-207.

30. T. Yin, Y. Wang, X. Chu, Y. Fu, L. Wang, J. Zhou, X. Tang, J. Liu, M. Huo, Free Adriamycin-Loaded pH/Reduction Dual-Responsive Hyaluronic Acid-Adriamycin Prodrug Micelles for Efficient Cancer Therapy. *ACS Applied Materials & Interfaces*, *10*(2018)35693-35704.

Table 1. Critical aggregation concentrations (CAC), Degree of substitution (DS), drug loading (DL), zeta potential, and encapsulation efficiency (EE) of the series of OSA-inulin micelles with diverse DPs in this work.

Sample	DP	DS (%)	Substituents per molecule	CAC (%)	Zeta potential without DOX (mV)	Zeta potential with DOX (mV)	EE (%)	DL (%)
H25P	2-8 (Evans *et al*., 2014)	33.3	~1.73	0.06±0.005	-51.9±1.05	-28.7±1.09	84.9±0.76	14.2±0.48
DS2	2-18 (Han *et al*., 2017)	30.7	~3.20	0.04±0.005	-55.9±2.18	-33.27±1.18	90.7±0.98	15.1±0.56
XL	20-23 (Ronkart, et al., 2007)	33.3	~7.00	0.02±0.005	-31.4±0.89	-7.68±0.89	95.6±1.42	15.9±0.92

Figure legends

Fig. 1. (A) Morphology of OSA-inulin and OSA-inulin-DOX micelles observed by TEM. Scale bar: 200 nm; (B) Zeta potentials of OSA-inulin micelles and OSA-inulin-DOX drug-loaded micelles determined by DLS (n=3, mean ± SD); (C) Encapsulation efficiency (EE) and drug loading (DL) of OSA-inulin-DOX micelles determined through UV/vis spectrophotometer (n=3, mean ± SD).

Fig. 2. (A) Hemolysis rates of Tween 80 and OSA-inulin micelles at different concentrations after incubation for 4 h and 12 h (n=3, mean ± SD); (B) Pictures of OSA-inulin micellar hemolysis; (C) Cytotoxicity of OSA-inulin micelles and OSA-inulin-DOX micelles against MCF-7 cells incubated for 72 h (n=5, mean ± SD).

Fig. 3. The uptake rate into MCF-7 cells of free DOX compared with those of OSA-inulin-DOX micelles (H2B-DOX, DS2-DOX, and XL-DOX) (A) FACS analysis. (B) CLSM images. Nuclei were stained blue with DAPI. Scale bar: 50 μm.

Fig. 4. *In vivo* antitumor effect of OSA-inulin-DOX micelles. (A) Images of tumors treated with free DOX and OSA-inulin-DOX micelles in comparison to the control (5 samples in each group); (B) Tumor volume *vs*. time graph (n = 5, mean ± SD) (**P＜0.01, ***P＜0.001); (C) Mice body weight changes during treatment (n = 5, mean ± SD) (***P＜0.001); (D) *In vivo* distribution images of OSA-inulin-DOX micelles and free DOX at 4 h and 24 h following the injection; (E) Tumor weights of mice at the end of the experiment (n = 5, mean ± SD) (*P＜0.05, ***P＜0.001); (F) Mice organ weights at the end of the experiment (n = 5, mean ± SD) (*P＜0.05).

Fig. 5. *In vivo* safety evaluation. (A) Serum index including ALT, AST, BUN, CRE

(*P＜0.05, ***P＜0.001); (B) Blood counts comprising white blood cells (WBC), red blood cells (RBC), platelets (PLT), and hemoglobin (HGB) (**P＜0.01, ***P＜0.001); (C) Pathological sections of H&E staining excised from the nude mice 1 month following the administration of diverse formulations.

Figures

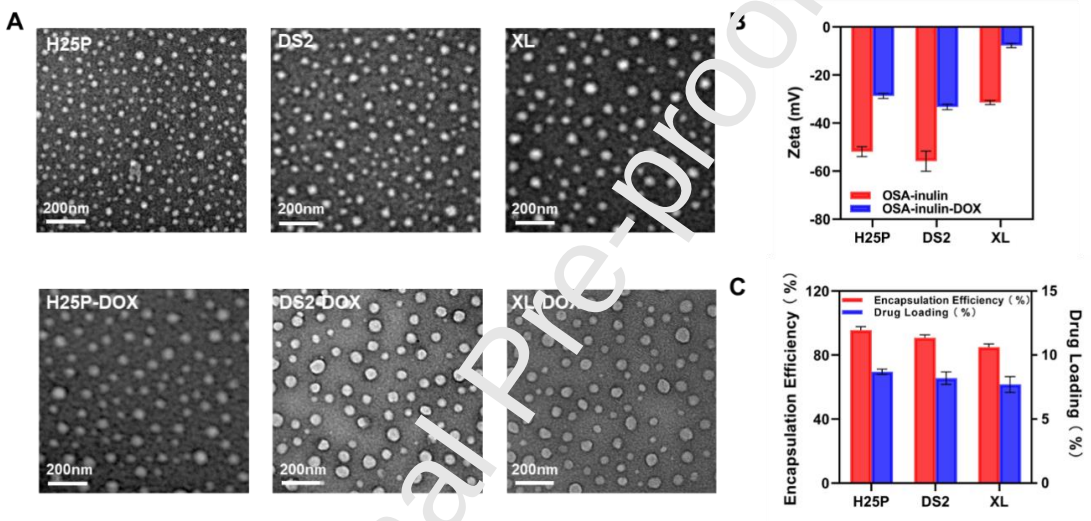

Fig. 1

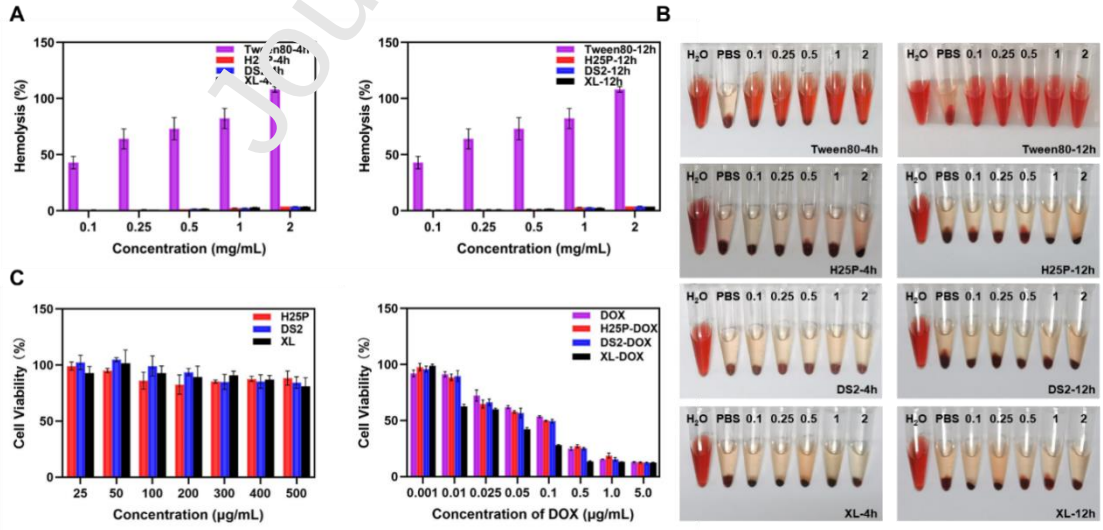

Fig. 2

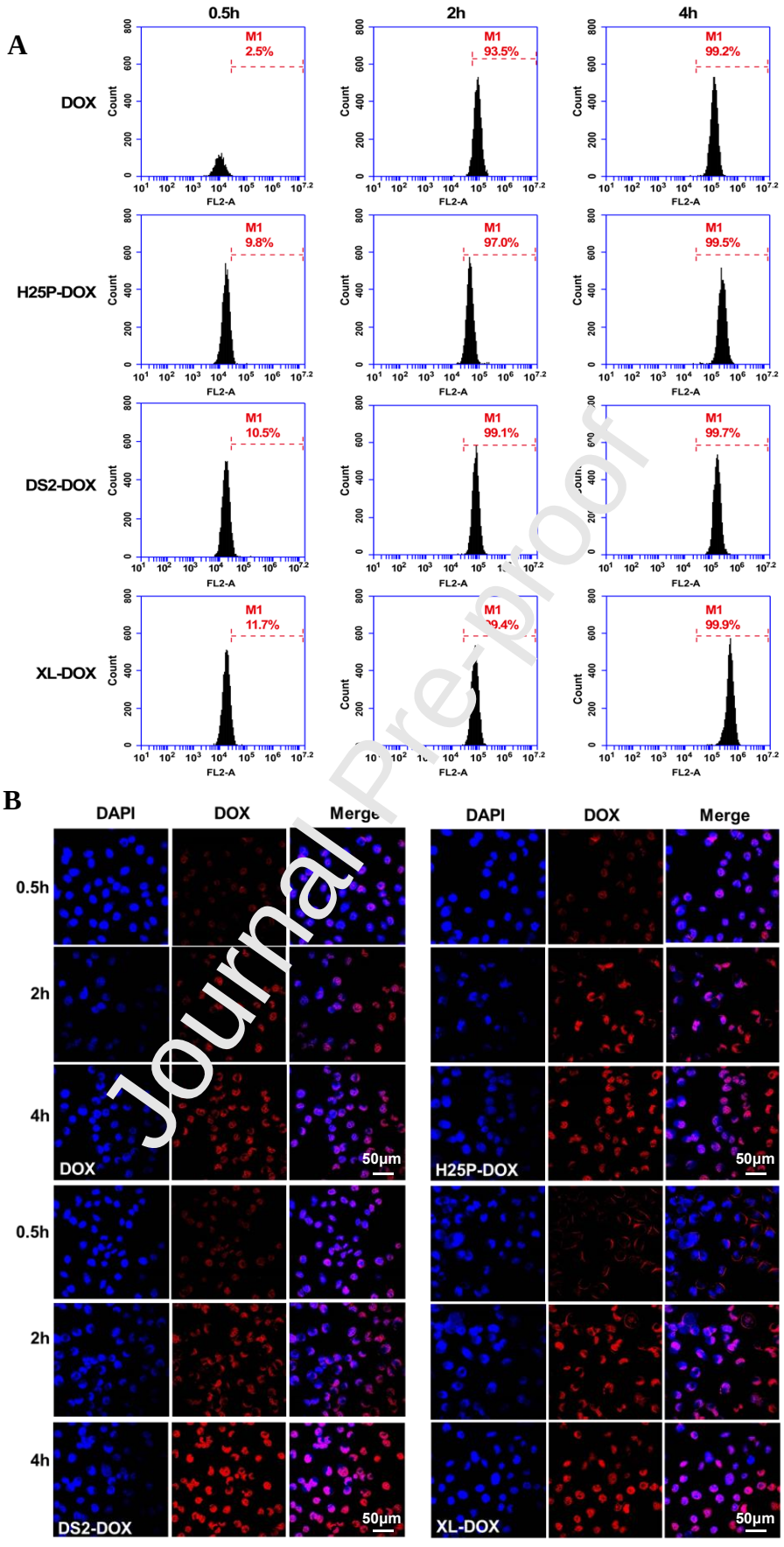

Fig. 3

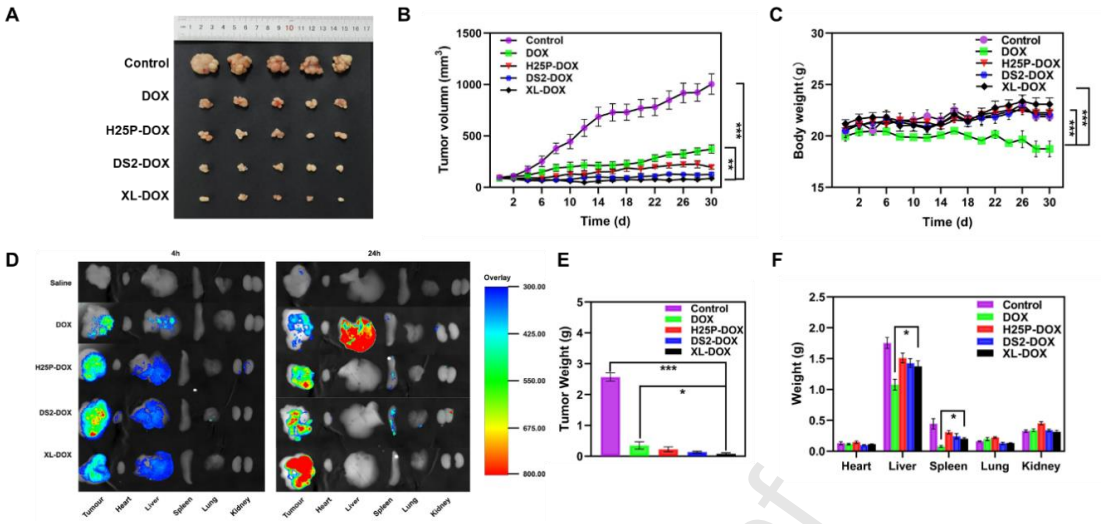

Fig. 4

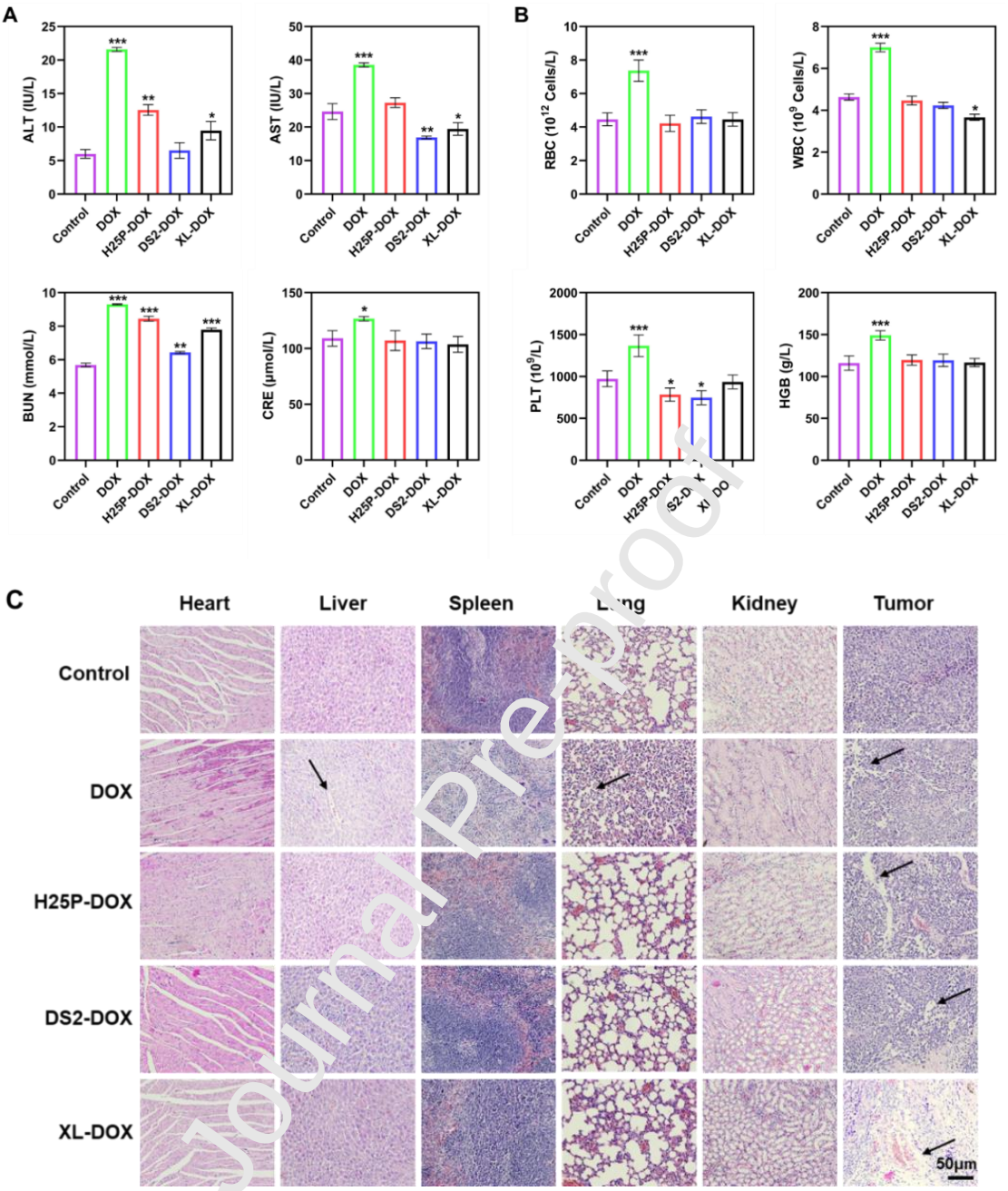

Fig. 5

Author Statement

Lingyu Han: Methodology, Formal analysis, Investigation, Writing-original draft, Writing review and editing

Jiao Sun: Methodology, Investigation, Writing-original draft, Writing review and editing

Peter A. Williams: Conceptualization, methodology, formal analysis, Writing review and editing

Jixin Yang: Conceptualization, methodology, Writing review and editing

Shubiao Zhang*: Conceptualization, methodology, Writing-original draft, Writing review and editing

Declaration of competing interest

The authors declare that they have no conflicts of interest regarding this work.

Highlights

1) The OSA-inulins formed micellar aggregates in aqueous solution and were able to solubilize doxorubicin.
2) OSA-inulin micelles efficiently encapsulate and deliver doxorubicin.
3) OSA-inulin-DOX micelles can strongly hindered tumor growth and and metastasis.
4) OSA-inulin-DOX micelles showed substantially lower systemic toxicity.